Title

Minimal Hammerhead Ribozymes with Uncompromised Catalytic Activity

Authors

O'Rourke, SM
Estell, W
Scott, WG

Publication Date

2015-02-04

DOI

10.1016/j.jmb.2015.05.005

Peer reviewed

Communication

Minimal Hammerhead Ribozymes with Uncompromised Catalytic Activity

Sara M. O'Rourke, William Estell and William G. Scott

Department of Chemistry and Biochemistry and The Center for the Molecular Biology of RNA, *University of California at Santa Cruz, Santa Cruz, CA 95064, USA*

Correspondence to William G. Scott: *wgscott@ucsc.edu*
http://dx.doi.org/10.1016/j.jmb.2015.05.005

Edited by P. C. Bevilacqua

Abstract

We report here that a single additional *trans*-Hoogsteen base-pairing interaction in the minimal hammerhead ribozyme transforms an RNA sequence possessing typically modest catalytic activity into one possessing greatly enhanced catalytic activity that is instead typical of full-length natural hammerhead RNAs that have additional extensive tertiary contact interactions. Formation of this additional base-pairing interaction requires only that the substrate RNA sequence contains a U at a position seven nucleotides 3′ to the cleavage site. No additions or changes are required in the minimal hammerhead ribozyme enzyme strand sequence (providing that the naturally occurring GUGA tetraloop of Stem II is maintained). This finding unambiguously demonstrates that a single Hoogsteen base-pairing interaction, in full-length hammerheads possessing this interaction, is sufficient for stabilizing the ribozyme active site, including alignment of the attacking nucleophile for the required inline hammerhead ribozyme reaction mechanism. This finding also implies that the idiosyncratic arrays of additional tertiary contacts observed in all naturally occurring full-length hammerhead sequences have evolved to prevent deleterious alternative pairing interactions within the context of the variety of natural sequences arising *in vivo*. Finally, this finding greatly simplifies and rationalizes the design of fast-cleaving engineered synthetic ribozymes as RNA nucleolytic reagents and as subjects for enzyme kinetics and mechanistic investigations.

Hammerhead RNAs are small autocatalytic motifs found within satellite RNAs of various plant RNA virus genomes [1,2], within the 3′-UTRs (*un*translated *r*egions) of various mammalian mRNAs [3], and within introns of many eukaryotes [4]. The hammerhead RNA catalyzes a self-cleavage reaction via phosphodiester isomerization that involves nucleophilic attack of the C17 2′O upon the adjacent scissile phosphate, producing 2′,3′-cyclic phosphate and 5′-hydroxyl termini in the cleavage product [5,6]. The reaction is in essence the same as the first step of that catalyzed by RNase A. Due to its small size, well-characterized reaction chemistry, known high-resolution three-dimensional structure [7], and intensive biophysical and biochemical investigation, as well as its widespread distribution [8], the hammerhead RNA is an ideal model system for understanding the most fundamental aspects of the chemistry of ribozyme catalysis [9].

A minimal hammerhead ribozyme construct consists of a conserved core of 15 mostly invariant residues [10]. Optimized minimal hammerhead ribozymes typically cleave with a rate of about 1/min under standard single-turnover conditions [11,12] (i.e., 10 mM Mg^{2+}, pH 7.5). In contrast, catalytically uncompromised full-length hammerhead ribozymes derived from natural sequences that include an array of tertiary contacts between loops in Stems I and II may experience up to a 100-fold rate enhancement compared to corresponding minimal hammerhead sequences [13–15]. X-ray crystal structures of two different classes of full-length natural hammerheads (Fig. 1) reveal two very different sets of these tertiary interactions [16,17]. Despite the differences, both sets of tertiary contacts have the same net effect of stabilizing the active-site structure in the conformation required for catalysis, with the general base (G12) poised to abstract the 2′-proton of C17 to activate the nucleophile positioned for inline attack [18].

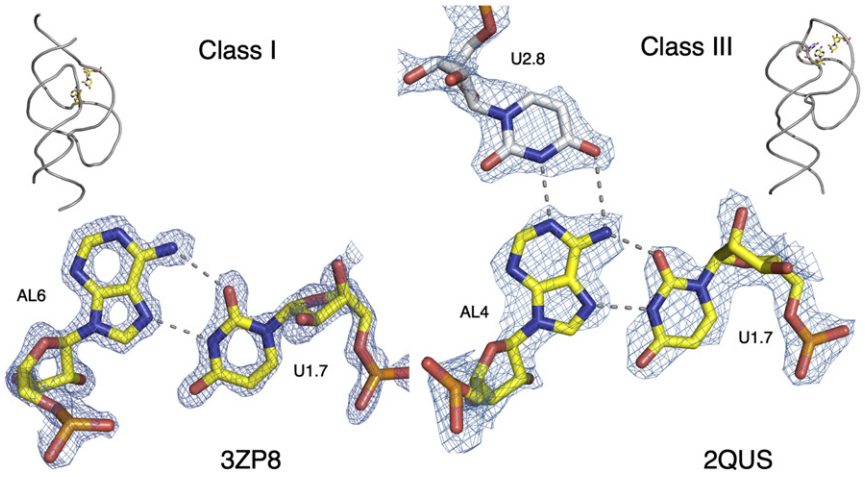

Fig. 1. Crystal structures of full-length Class I and Class III hammerhead ribozymes. A Class I hammerhead ribozyme structure (3ZP8), shown on the left side of the figure, was obtained at 1.55 Å resolution [7], enabling the location of all nonhydrogen atoms to be clearly defined. The gray ribbon structure in the top left depicts the backbone fold in which a conserved *trans*-Hoogsteen AU pair within the tertiary contact region between Stem–loop II and Stem I is highlighted in yellow. A close-up of the *trans*-Hoogsteen AU pair, conserved in the Smα1 and mammalian 3′-UTR hammerheads, is shown in the context of a defining $2F_o - F_c$ electron density map (indicated as a blue-gray mesh) contoured at 2.0 r.m.s.d. A Class III hammerhead ribozyme structure (2QUS), shown on the right side of the figure, was obtained at 2.4 Å resolution [17]. The gray ribbon structure in the top right depicts the backbone fold in which a conserved *trans*-Hoogsteen AU pair within the tertiary contact region between Stem–loop II and Stem–loop I is highlighted in yellow, and an additional U (2.8) participating in a Watson–Crick pairing interaction with the A, shown in white, forms a base triple. A close-up of the base triple that includes the *trans*-Hoogsteen AU pair, conserved in many Class III hammerheads as described in the text, is shown in the context of a defining $2F_o - F_c$ electron density map (indicated as a blue-gray mesh) at 1.8 r.m.s.d. The conserved *trans*-Hoogsteen AU pair is the only structural feature the Class I and Class III hammerhead tertiary contacts share in common.

Unlike the mostly invariant sequence of the minimal hammerhead RNA catalytic core, there is little apparent sequence conservation within the tertiary contact regions of the more catalytically active full-length hammerhead RNAs [8,14]. For this reason, the existence of the tertiary contact remained undetected until 16 years after the discovery of the hammerhead ribozyme.

The two most frequently occurring groupings of natural hammerhead RNAs are the Class I hammerheads and the most common subset of Class III hammerheads. Class I hammerheads are defined as those lacking a connecting loop on Stem I, and Class III hammerheads are those lacking a connecting loop on Stem III [19]. Class I hammerhead RNAs include the Smα1 hammerhead discovered in *Schistosoma mansoni* [20] and a collection of discontinuous hammerhead sequences found embedded within the 3′-UTRs of mammalian mRNAs [3]. Class III hammerheads include the first hammerhead discovered, that embedded within the genomic strand of the satellite RNA of tobacco ringspot virus (sTRSV+) [1], and those of related plant virus-associated RNA sequences [21].

Class I hammerheads and Class III hammerheads have quite different tertiary contacts, in terms of both sequence and structure, due in part to the differences in backbone connectivity. Class I hammerheads have a set of tertiary interactions between a six-nucleotide connecting loop on Stem II and a internal bulge within Stem I. The most frequently occurring subset of Class III hammerheads has a set of tertiary interactions between a (typically) four-nucleotide connecting loop on Stem II and connecting loop of variable size on Stem I. Crystal structures of both Class I and Class III hammerheads are available [7,16,17]. Representative structures from both classes are shown in Fig. 1. The Class I hammerhead structure, obtained from a sequence derived from the Smα1 hammerhead at 1.55 Å resolution [7], is shown as a backbone representation on the left, and the Class III hammerhead structure, obtained from a sequence derived from the sTRSV+ hammerhead at 2.4 Å resolution [17], is shown as a backbone representation on the right. Although the catalytic core regions of both classes of hammerheads are essentially identical [17], the tertiary contact regions are distinctly different.

The *only* interaction that the two classes of hammerhead RNAs share in common is a *trans*-Hoogsteen AU base pair [22], shown in both structures as an all-nonhydrogen-atom stick figure in the context of the defining electron density, in which the carbon atoms are colored yellow (Fig. 1). In the case of the sTRSV+ hammerhead, the *trans*-Hoogsteen base pair is part of a base triple [17] (in which an additional U, indicated

with white carbons in Fig. 1, forms a Watson–Crick pair with the A). In addition to the *Schistosoma* hammerhead, all of the discontinuous hammerheads found embedded in mammalian 3′-UTRs have a U at position 1.7 and an A at the sixth position of the Stem II loop [3], indicating that the observed *trans*-Hoogsteen AU base-pairing tertiary contact is conserved in Class I hammerheads. In addition to the sTRSV+ hammerhead, nine of twelve hammerheads presented in a paper originally identifying the hammerhead tertiary interactions [14] have a U at 1.7, and all possess AL4 in Stem II, suggesting conservation of the *trans*-Hoogsteen AU pair in sTRSV+-like Class III hammerheads; the remaining three have C1.7, which can form an equivalent *trans*-Hoogsteen AC pair if the C is protonated. (An additional more recently discovered subset of Class III hammerheads does not have a sequence conservation pattern indicating the presence of a *trans*-Hoogsteen AU pair and is instead believed to have a novel pseudoknot tertiary contact [23].)

In this paper, we report the finding that a minimal hammerhead ribozyme sequence, in which U1.7 is present in the substrate strand and AL4 is present in Stem–loop II of an enzyme strand truncated at position 2.6 (to prevent interference with the formation of the conserved AL4–U1.7 pairing interaction observed in the Class I and Class III hammerheads), possesses the catalytic activity of the corresponding full-length hammerhead ribozyme. The primary significance of this finding is twofold: Firstly, fast-cleaving hammerhead ribozymes can be designed easily without the need to incorporate any of the complex and nonconserved tertiary interactions observed in the various crystal structures. Secondly, the results of our control and rescue experiments permit us to suggest that the nonconserved tertiary interactions in the full-length natural hammerhead sequences serve primarily to prevent the formation of deleterious conformations that inhibit formation of the AL4–U1.7 pairing interaction.

The following nine experiments establish that the AL4–U1.7 interaction found in the Class I and Class III full-length hammerhead ribozyme crystal structures (Fig. 1) is alone both necessary and sufficient for most the enhanced catalytic activity observed in the context of full-length Class I and Class III hammerhead ribozymes that possess the conserved *trans*-Hoogsteen AU pair.

Experiment 1 employs the minimal hammerhead ribozyme construct shown in Fig. 2a, in which the

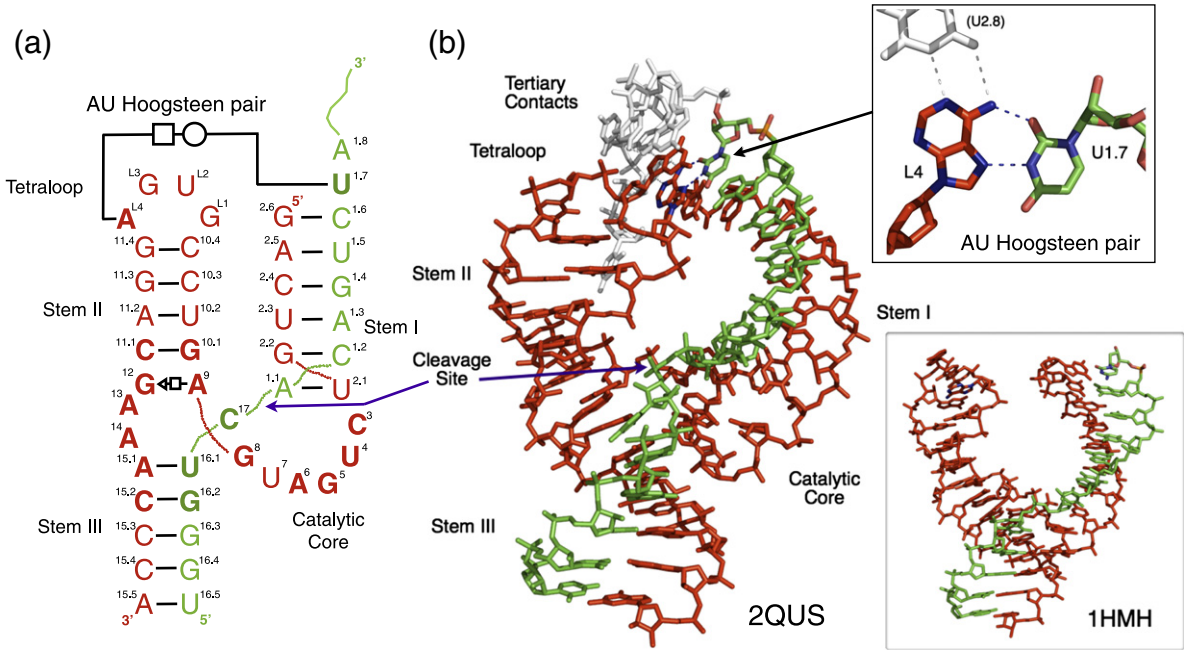

Fig. 2. (a) A secondary structure representation of the minimal ribozyme $HH_{min\text{-}AL4:U1.7}$ (Experiment 1 in Table 1) with high activity. The enzyme strand is shown in red; the substrate is in green. The cleavage site is indicated with a blue arrow. Invariant and conserved nucleotides in the catalytic core are highlighted in boldface, as is AL4 in the tetraloop and U1.7 in Stem I. The numbering scheme is standardized [26]. (b) The corresponding proposed three-dimensional structure, using the same color scheme, based on the coordinates designated 2QUS [17] in the PDB. The AU *trans*-Hoogsteen base pair is shown as a close-up in the box in the upper right side of the figure. Nucleotides involved in the elaborate tertiary contact present in 2QUS, but absent in the sequence shown in (a), are indicated as light gray, including U2.8, which forms a base triple with the AU Hoogsteen pair. The inset in the lower right shows the corresponding minimal hammerhead ribozyme as observed in the original crystal structures, including 1HMH [25]. In this case, there are no stabilizing contacts between the tetraloop on the left side of the molecule and Stem I on the right side.

5′-end of the enzyme strand terminates at position 2.6, enabling AL4 to form a *trans*-Hoogsteen base pair with U1.7 as observed in all of the Class I and Class III hammerhead full-length ribozyme crystal structures (Figs. 1 and 2b). The observed rate constant of 0.77/min at pH 5.6 (Table 1 and Fig. 3) is similar to that observed for a full-length sTRSV + hammerhead RNA [24] (Experiment B in Table 1) and is greater than that for a two-stranded ribozyme construct derived from the same sTRSV + sequence [24] (Experiment A in Table 1). The result of this experiment demonstrates that the AL4–U1.7 pairing interaction is, by itself, sufficient for the enhanced catalytic activity characteristic of the full-length sTRSV +-like Class III hammerheads.

Experiment 2 is a negative control designed to demonstrate that the AL4–U1.7 pairing interaction is responsible for the observed catalytic enhancement relative to a typical minimal hammerhead. The 5′-end of the enzyme strand sequence of Experiment 1 was extended beyond position 2.6 to form eight additional canonical Watson–Crick base pairs in Stem I with U1.7 through G1.15 of the substrate (S_1 in Table 1), thus preventing formation of the AL4–U1.7 pairing interaction. The resulting minimal hammerhead extends the Stem I A-form helix (Fig. 2b, lower inset) [25]. This construct serves as an important control, as it displays typical minimal hammerhead ribozyme kinetics (compare to Experiment C, in Table 1, in which $HH_{16\text{-min}}$ is a standard, well-characterized minimal hammerhead) [24].

Experiment 3 employs the hammerhead sequence of Experiment 1 with the addition of a 5′-GUU sequence. The 5′-GUU sequence was initially designed to enable formation of the base triple (Fig. 1, bottom right) observed in the Class III hammerhead crystal structures [17], with the intent of further enhancing the catalytic activity. Instead, the presence of these three additional nucleotides apparently partially interferes with the AL4–U1.7 base-pairing interaction, resulting in a hammerhead approximately 10-fold more active than the minimal hammerhead and significantly less active than the hammerhead sequence from Experiment 1.

Experiment 4 employs the hammerhead sequence of Experiment 1 in which the G in the third position of the tetraloop capping Stem II is replaced with an A. This hammerhead is only marginally more active than the control minimal hammerhead in Experiment 2, suggesting that AL3 deleteriously competes with AL4 for pairing with U1.7.

Experiment 5 is similar to Experiment 4, but the GL3A mutation is replaced with a GL3U mutation. This hammerhead, in contrast to that of Experiment 4, is at least as active as the sequence in Experiment 1, suggesting that UL3 (unlike AL3) cannot compete with AL4 for pairing with U1.7.

Experiment 6 combines Experiment 3 with Experiment 4. Although each change by itself is deleterious, combining the two changes rescues the ribozyme, restoring full catalytic activity, suggesting that the presence of the 5′-GUU sequence sequesters AL3, preventing it from competing with the formation of the AL4–U1.7 pairing interaction. Similarly, AL3 prevents the 5′-GUU sequence from interfering with the AL4–U1.7 pairing interaction.

Experiment 7 combines Experiment 3 with Experiment 5. Again, full catalytic activity is restored, demonstrating that a nucleotide at position L3 can rescue ribozyme activity by preventing the deleterious 5′-GUU interference observed in Experiment 3.

Experiment 8 replaces AL4 with a C in the sequence of Experiment 1. With CL4 adopting the *syn*-conformation, a parallel CU base-pairing interaction, isostructural with respect to an AU *trans*-Hoogsteen base pair, is maintained without requiring perturbation of the positions of either ribose moiety or the adjacent phosphates. This control, which is only twofold less active than the sequence in Experiment 1, is consistent with the *trans*-Hoogsteen AU pairing interaction observed in the Class I and Class III hammerhead crystal structures and is inconsistent with possible aberrant alternative pairing interactions between AL4 and U1.7, such as reverse Watson–Crick pairing.

Experiment 9 is analogous to Experiment 1 but involves a minimized hammerhead ribozyme sequence derived from the Smα1-like 3ZP8-crystallized hammerhead sequence, maintaining the crystallographically observed AL6–U1.7 *trans*-Hoogsteen base pair. Again, the 5′-end of the enzyme strand terminates at position 2.6. This hammerhead sequence is 2.5-fold less active than the sequence assayed in Experiment 1 and about twofold less active than the originally crystallized 3ZP8 sequence [16]. This control demonstrates that our experimental observations focused on the sTRSV +-like Class III ribozymes are generalizable to the Class I hammerheads as well. (The only remaining substantive difference between this minimized sequence and that of Experiment 1 is the six-nucleotide Stem–loop II *versus* the four-nucleotide Stem–loop II of the sTRSV +-like ribozymes.)

In summary, we have observed two unanticipated properties of the catalysis-enhancing tertiary contact interactions found in many of the natural full-length hammerhead RNAs.

First, we have found that as long as the *trans*-Hoogsteen pair between U1.7 and AL4 observed in the Class I and Class III hammerhead crystal structures is maintained, all of the other tertiary contacts between Stems I and II, including the participation of U2.8 in the base triple (Fig. 1), can be eliminated without compromising the enhanced catalytic activity of the ribozyme. Consequently, a minimal hammerhead enzyme strand constructed with a 5′-end beginning exactly at position 2.6 (Fig. 2a), targeting a substrate with U1.7, will enable pairing between AL4 and U1.7 without interference or competition, as shown in Fig. 2b.

Table 1. Single-turnover kinetics for sTRSV-like hammerhead ribozymes: Integrated rate equation curve-fitting parameters

Number	$HH_{construct}$	Experiment	k_{obs} at pH 5.6 (min^{-1})	k_{obs} at pH 6 (min^{-1})	k_{obs} at pH 7.5 (min^{-1})	Fraction cleaved		RNA sequences assayed (5′ to 3′)
						F_o	F_{sat}	
1	$HH_{min\text{-}AL4:U1.7}$	Original sequence with *trans*-Hoogsteen AU tertiary base pair observed in all full-length hammerhead crystal structures	0.77 ± 0.11	1.9 ± 0.3[a]	61. ± 9.[a]	0.11	0.90	GACUGUCUGAUGAGUCC**GUGA**G GACGAAACCCA
2	$HH_{min\text{-}WC\text{-}AU}$	Negative control: Minimal Hammerhead that blocks formation of the *trans*-Hoogsteen AU tertiary base pair	0.02 ± 0.01[a]	0.05 ± 0.01[a]	1.5 ± 0.2	0.15	0.69	**GGCCCAUAAUA**GACUGUCUGAUG AGUCC**GUGA**GGACGAAACCCA
3	$HH_{min\text{-}5'GUU}$	Negative control: 5′GUU competes with *trans*-Hoogsteen AU tertiary base-pair formation	0.19 ± 0.03	0.48 ± 0.07[a]	15. ± 2[a]	0.14	0.88	**GUU**GACUGUCUGAUGAGUCC**GUG A**GGACGAAACCCA
4	$HH_{min\text{-}GL3A}$	Negative control: GL3A mutation reduces cleavage rate by competing with AL4 for U1.7 pairing	0.063 ± 0.02	0.15 ± 0.05[a]	5.0 ± 1.6[a]	0.07	0.50	GACUGUCUGAUGAGUCC**GUAA**G GACGAAACCCA
5	$HH_{min\text{-}GL3U}$	Positive control: GL3U mutation does not compete with AL4 for U1.7 pairing	1.2 ± 0.2	3.0 ± 0.6[a]	95. ± 20[a]	0.11	0.53	GACUGUCUGAUGAGUCC**GUUA**G GACGAAACCCA
6	$HH_{min\text{-}GL3A\text{-}5'GUU}$	Positive control: GL3A mutation rescues ribozyme by preventing 5′GUU competing with *trans*-Hoogsteen AU tertiary base-pair formation	1.0 ± 0.2	2.5 ± 0.6[a]	79 ± 20[a]	0.05	0.76	**GUU**GACUGUCUGAUGAGUCC**GUA A**GGACGAAACCCA
7	$HH_{min\text{-}GL3U\text{-}5'GUU}$	Positive control: GL3U mutation rescues ribozyme by preventing 5′GUU competing with *trans*-Hoogsteen AU tertiary base-pair formation	1.2 ± 0.2	3.0 ± 0.6[a]	95. ± 20[a]	0.10	0.68	**GUU**GACUGUCUGAUGAGUCC**GU UA**GGACGAAACCCA
8	$HH_{min\text{-}AL4C:U1.7}$	Positive control: Original sequence with parallel CU pair isostructural with respect to the *trans*-Hoogsteen AU tertiary base pair	0.39 ± 0.03	0.96 ± 0.07[a]	31. ± 2[a]	0.04	0.40	GACUGUCUGAUGAGUCC**GUGC**G GACGAAACCCA
9	$HH_{3zp8\text{-}min\text{-}AL4:U1.7}$	Positive control: Minimized version of crystallized 3ZP8 (a *Schistosoma*-type hammerhead sequence) with 5′-terminus at U2.6	0.30 ± 0.05	0.74 ± 0.12[a]	24. ± 4[a]	0.03	0.55	UACCAGCUGAUGAGUCC**CAA AUA**GGACGAAACGCC
S	$HH_{substrate1}$	Substrate for hammerhead sequences 1–7						*Cye3*_UGG**GUC**ACAGUC**U**AUUAUGGG
S′	$HH_{substrate8}$	Substrate for hammerhead sequence 8 (from 3ZP8)						*Cye3*_GGC**GUC**CUGGUA**U**CCAAUCC
A	$HH_{16\text{-}T1}$ [19]	External control: Previously reported two-stranded hammerhead derived from sTRSV+ preserving all natural tertiary contacts	0.25[a]	0.62[b]	20.[a]	(Previously published values [19] are provided as external controls.)		
B	$HH_{16\text{-}T2}$ [19]	External control: Previously reported single-stranded hammerhead derived from sTRSV+ preserving all natural tertiary contacts	0.76[a]	1.9[b]	60.[a]			
C	$HH_{16\text{-}min}$ [19]	External control: Previously reported kinetically well-behaved minimal hammerhead ribozyme	0.01[a]	0.03[a,b]	1.[c]			

The first nine entries in the table are the hammerhead ribozyme enzyme strands assayed for cleavage activity. Nucleotides added to the 5′-end of the second, third, sixth, and seventh hammerhead enzyme strands are highlighted in boldface, as are the nucleotide sequences of Stem–loop II. The 11 nucleotides added to the 5′-end of the second hammerhead (a minimal hammerhead negative control) are designed to extend Stem I by forming Watson–Crick base pairs involving U1.7 through G1.15 of the substrate, thus locking it into a conventional minimal hammerhead structure that is incompatible with formation of the U1.7-AL4 *trans*-Hoogsteen pair. Minimal hammerheads in Experiments 3, 6, and 7 have an added 5′-GUU sequence that has the potential to form additional tertiary contacts, including a base triple, U1.7-AL4-U2.8, shown in Figs. 1 and 2. The 10th row of the table shows the substrate strand (S) used for each of the single-turnover ribozyme assays in Experiments 1–8, and the next row shows the substrate sequence (S′) used in Experiment 9. The previously recognized substrate cleavage consensus sequence, GUC, is shown in boldface in rows S and S′, as well as U1.7 that participates in the *trans*-Hoogsteen pair. Results reported without a superscript annotation were calculated from primary data obtained at the indicated pH using the single-turnover procedure described previously [12]. The final three entries in the table (Experiments A, B, and C) are provided as external controls, that is, previously published results from another laboratory [11,24] that have thoroughly characterized hammerhead ribozymes derived from the sTRSV+ natural hammerhead ribozyme. We have extrapolated rate constants to two additional pH conditions, using $k_{obs(extrapolated)} = k_{obs} \times 10^{\Delta pH}$ as previously described [19] to facilitate comparison. The values reported for Experiment C serve as an internal consistency check for this method of extrapolation.

[a] Extrapolated rate constant, using $k_{obs(extrapolated)} = k_{obs} \times 10^{\Delta pH}$ as previously described [24].

[b] k_{obs} values calculated using $k_{obs} = (k_{+2} + k_{-2})$, where $k_{\pm 2}$ are reported rate constants [24].

[c] Observed reported rate constant [11].

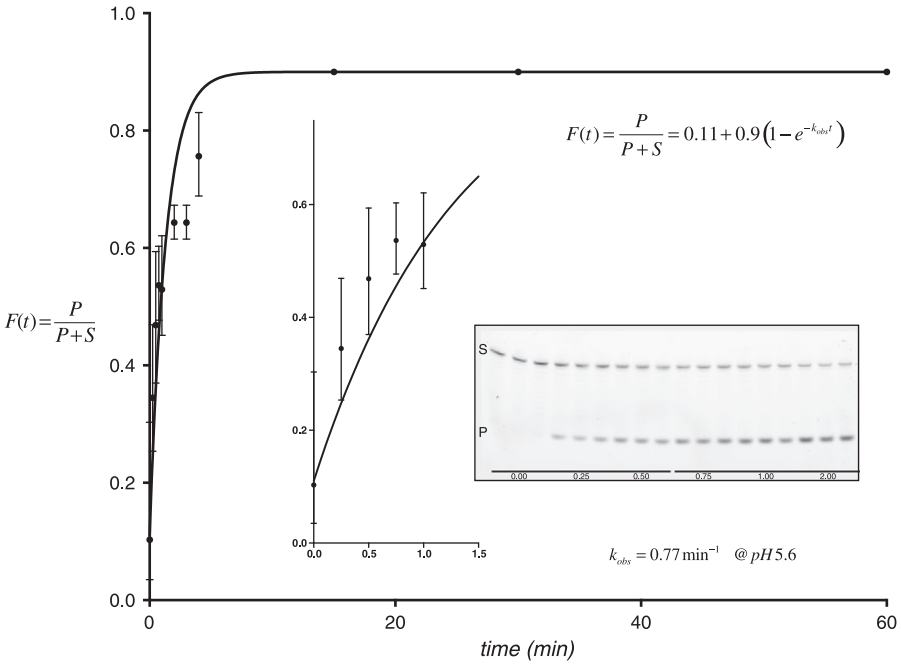

Fig. 3. Representative single-turnover kinetic data for the minimal ribozyme with high activity ($HH_{min\text{-}AL4:U1.7}$) shown in Fig. 2a and summarized in the first row (Experiment 1) of Table 1. The fraction of product produced as a function of time, $F(t)$, was quantified in triplicate by polyacrylamide gel electrophoresis separation of fluorescently labeled substrate and product (gel inset). The data were fit to a single standard exponential function [11,12], where F_o = 0.11 is the initial fraction of cleavage product and F_{sat} = 0.9 is the estimated extent of cleavage based upon the final three time points. Nonlinear regression analysis was performed to estimate k_{obs}, as described in the experimental methods. The most conservative estimate for k_{obs} is 0.77/min at pH 5.6, which is essentially the same as k_{obs} for an optimized one-stranded full-length hammerhead based on the sTRSV+ natural full-length hammerhead RNA sequence ($HH_{16\text{-}T2}$) [24], as shown in Experiment B in Table 1. The graph inset expands the initial time points of the dataset. (The data were also fit to a more complex kinetic model with an unrestrained two-phase exponential function, producing an estimated fast-phase k_{obs} of 3.6 ± 1.5/min corresponding to the initial time points in the inset and a slower phase of 0.2 ± 0.1/min, with unrestrained endpoints of F_o = 0.11 ± 0.01 and F_{sat} = 0.91 ± 0.05.)

Minimal intermolecular hammerhead ribozymes that begin at position 2.6 and possess the natural sTRSV+ Stem–loop II sequence ($HH_{min\text{-}AL4:U1.7}$) have essentially the same enhanced catalytic activity (Fig. 3 and Experiment 1 in Table 1) previously observed only in optimized full-length sTRSV-derived hammerhead constructs ($HH_{16\text{-}T2}$) and significantly greater activity than the corresponding nonoptimized sequences ($HH_{16\text{-}T1}$) [24] (Experiments A and B in Table 1). Experiment 8, in which a comparatively drastic AL4C mutation preserves much of the catalytic enhancement, experimentally corroborates the assumption that the conserved *trans*-Hoogsteen AL4–U1.7 interaction observed in the Class I and Class III full-length hammerhead crystal structures is present in the minimal hammerhead construct with enhanced activity. CL4 in the *syn*-conformation enables formation of a parallel CU pair, in which the hydrogen bond donor and acceptor of CL4 are isosteric with those on the Hoogsteen face of AL4, consistent with the conserved *trans*-Hoogsteen AL4–U1.7 interaction (Supplementary Fig. A) and inconsistent with other potential base-pairing interactions. Experiment 9, in which a similarly minimized Class I hammerhead is also shown to have significantly enhanced catalytic activity, further establishes that our observation is generalizable.

Second, we have also found that all of the nonconserved tertiary interactions in the full-length hammerhead (i.e., all of those apart from the *trans*-Hoogsteen AU pair) appear to exist primarily to prevent deleterious alternative interactions from taking place that may potentially interfere with the *trans*-Hoogsteen pair formation. In particular, the 5′-GUU and GL3A modifications (Experiments 3 and 4 in Table 1) by themselves are each significantly deleterious presumably because they interfere or compete with the formation of the AL4–U1.7 interaction. However, when the two modifications are combined (Experiment 6 in Table 1), the enhanced ribozyme activity is fully rescued. Based upon the crystal structure of the active, full-length hammerhead, the 5′G is predicted to form a single hydrogen bond with GL3 in $HH_{min\text{-}5'GUU}$, (Experiment 3 in Table 1), which is likely not enough to prevent formation of an alternative, inhibitory conformation

that may (imperfectly) extend Stem I, preventing formation of the Hoogsteen pair. Additionally substituting the G at the L3 position with an A potentially provides a second hydrogen bond between the Hoogsteen faces of both purines, which apparently rescues k_{+2} (the forward or cleavage rate constant) and enhances k_{-2} (the reverse or ligation rate constant) so that the overall k_{obs} increases from 0.77 min^{-1} to 1.0 min^{-1} and the fraction cleaved as equilibrium is approached decreases from 0.9 to 0.76 (Experiment 6 in Table 1). When G at position L3 is instead replaced with a U, a GU wobble pair can potentially form, which similarly rescues k_{+2} and enhances k_{-2} (Experiment 7 in Table 1).

Hence, it appears that the AL4–U1.7 *trans*-Hoogsteen base pair alone is responsible for increasing k_{+2} by over a factor of ~50 and that the increase in the ligation rate, $k_{-2,}$ as observed in the experimental controls, may be due to the increase in hydrogen bonding base-pairing contacts, whether they occur within the tertiary contact region of full-length hammerheads or simply as a result of extending Stem I in the case of minimal hammerheads.

We have demonstrated that the AL4–U1.7 *trans*-Hoogsteen base pair is both necessary and sufficient to confer the >50-fold enhanced cleavage activity (k_{+2}) characteristic of the full-length hammerhead ribozymes possessing extensive tertiary interactions that include the AL4–U1.7 *trans*-Hoogsteen base pair. The remaining tertiary interactions, which do not appear to adhere to any obvious sequence conservation patters, therefore most likely exist primarily to prevent deleterious alternative structures from forming that are incompatible with formation of the required *trans*-Hoogsteen pair but may also enhance the reverse reaction (albeit in a nonsequence-specific manner). If a minimal intermolecular hammerhead ribozyme is designed as an RNA cleavage reagent with this in mind, no need for designing the additional tertiary contacts ever arises. The design problem instead reduces quite simply and rationally to that of targeting substrates restricted to having a U at position 1.7. The fully active minimal enzyme strand can then be designed with a 5′-end exactly at position 2.6 and in such a way as to preserve the natural sTRSV+ hammerhead Stem–loop II GUGA sequence. In addition, the observation that some RNA tertiary structural interactions may function primarily to prevent deleterious alternative structural interactions from forming is likely generalizable to other structured RNAs.

Acknowledgement

This work is supported by the National Institutes of Health grant R01GM087721 to W.G.S.

Conflict of Interest Statement: No competing financial interests have been declared.

Appendix A. Supplementary data

Supplementary data to this article can be found online at http://dx.doi.org/10.1016/j.jmb.2015.05.005.

Received 4 February 2015;
Received in revised form 7 May 2015;
Accepted 8 May 2015
Available online 14 May 2015

Keywords:
hammerhead ribozyme;
RNA catalysis;
RNA tertiary contacts;
RNA structure;
ribozyme kinetics

References

[1] Prody GA, Bakos JT, Buzayan JM, Schneider IR, Breuning G. Autolytic processing of dimeric plant virus satellite RNA. Science 1986;231:1577–80.
[2] Forster AC, Symons RH. Self-cleavage of virusoid RNA is performed by the proposed 55-nucleotide active site. Cell 1987;50:9–16.
[3] Martick M, Horan LH, Noller HF, Scott WG. A discontinuous hammerhead ribozyme embedded in a mammalian messenger RNA. Nature 2008;454:899–902.
[4] García-Robles I, Sánchez-Navarro J, de la Peña M. Intronic hammerhead ribozymes in mRNA biogenesis. Biol Chem 2012;393:1317–26.
[5] Uhlenbeck OC. A small catalytic oligoribonucleotide. Nature 1987;328:596–600.
[6] Wedekind JE, McKay DB. Crystallographic structures of the hammerhead ribozyme: relationship to ribozyme folding and catalysis. Annu Rev Biophys Biomol Struct 1998;27:475–502.
[7] Anderson M, Schultz EP, Martick M, Scott WG. Active-site monovalent cations revealed in a 1.55-Å-resolution hammerhead ribozyme structure. J Mol Biol 2013;425:3790–8.
[8] Hammann C, Luptak A, Perreault J, de la Peña M. The ubiquitous hammerhead ribozyme. RNA 2012;18:871–85.
[9] Ferré-D'Amaré AR, Scott WG. Small self-cleaving ribozymes. Cold Spring Harb Perspect Biol 2010;2:a003574.
[10] Ruffner DE, Stormo GD, Uhlenbeck OC. Sequence requirements of the hammerhead RNA self-cleavage reaction. Biochemistry 1990;29:10695–702.
[11] Hertel KJ, Herschlag D, Uhlenbeck OC. A kinetic and thermodynamic framework for the hammerhead ribozyme reaction. Biochemistry 1994;33:3374–85.
[12] Stage-Zimmermann TK, Uhlenbeck OC. Hammerhead ribozyme kinetics. RNA 1998;4:875–89.
[13] De la Peña M, Gago S, Flores R. Peripheral regions of natural hammerhead ribozymes greatly increase their self-cleavage activity. EMBO J 2003;22:5561–70.

[14] Khvorova A, Lescoute A, Westhof E, Jayasena SD. Sequence elements outside the hammerhead ribozyme catalytic core enable intracellular activity. Nat Struct Biol 2003;10:708–12.
[15] Canny MD, Jucker FM, Kellogg E, Khvorova A, Jayasena SD, Pardi A. Fast cleavage kinetics of a natural hammerhead ribozyme. J Am Chem Soc 2004;126:10848–9.
[16] Martick M, Scott WG. Tertiary contacts distant from the active site prime a ribozyme for catalysis. Cell 2006;126:309–20.
[17] Chi Y-I, Martick M, Lares M, Kim R, Scott WG, Kim S-H. Capturing hammerhead ribozyme structures in action by modulating general base catalysis. PLoS Biol 2008;6:e234.
[18] Przybilski R, Hammann C. The hammerhead ribozyme structure brought in line. Chembiochem 2006;7:1641–4.
[19] Daub J, Gardner PP, Tate J, Ramsköld D, Manske M, Scott WG, et al. The RNA WikiProject: community annotation of RNA families. RNA 2008;14:1–3.
[20] Ferbeyre G, Smith JM, Cedergren R. Schistosome satellite DNA encodes active hammerhead ribozymes. Mol Cell Biol 1998;18:3880–8.
[21] Seehafer C, Kalweit A, Steger G, Gräf S, Hammann C. From alpaca to zebrafish: hammerhead ribozymes wherever you look. RNA 2011;17:21–6.
[22] Leontis NB, Westhof E. Geometric nomenclature and classification of RNA base pairs. RNA 2001;7:499–512.
[23] Jimenez RM, Delwart E, Lupták Andrej. Structure-based search reveals hammerhead ribozymes in the human microbiome. J Biol Chem 2011;286:7737–43.
[24] Nelson JA, Shepotinovskaya I, Uhlenbeck OC. Hammerheads derived from sTRSV show enhanced cleavage and ligation rate constants. Biochemistry 2005;44:14577–85.
[25] Pley HW, Flaherty KM, McKay DB. Three-dimensional structure of a hammerhead ribozyme. Nature 1994;372:68–74.
[26] Hertel KJ, Pardi A, Uhlenbeck OC, Koizumi M, Ohtsuka E, Uesugi S, et al. Numbering system for the hammerhead. Nucleic Acids Res 1992;20:3252.